

# **Reduction of brain metastases in plasminogen activator inhibitor-1 deficient mice with transgenic ocular tumors**

C. Maillard<sup>1</sup>, C. Bouquet<sup>2</sup>, M. Petitjean<sup>1</sup>, M. Mestdagt<sup>1</sup>, E. Frau<sup>2</sup>, M. Jost<sup>1</sup>, P. Opolon<sup>2</sup>, F. Beermann<sup>4</sup>, M. Abitbol<sup>3</sup>, J.M. Foidart<sup>1, 5</sup>, M. Perricaudet<sup>2</sup> and A. Noël<sup>1</sup>

1. Laboratory of Tumor and Development Biology, Centre de Recherche en Cancérologie Expérimentale (CRCE), CBIG, Tour de Pathologie (B23), Sart-Tilman; B-4000 Liège, University of Liège, Belgium;
2. CNRS UMR 8121 Univ Paris Sud, Vectorologie et Transfert de Gènes, Institut Gustave Roussy, 39 rue Camille Desmoulins, 94805, Villejuif, France;
3. CERTO, Faculté de Médecine Necker, 156 rue de Vaugirard, 75015 Paris, France;
4. Swiss Institute for Experimental Cancer Research (ISREC), Chemin de Boveresses 155, CH-1066 Epalinges, Switzerland;
5. Department of Gynecology and Obstetrics, CHU, Liège, Belgium.

Running title: PAI-1 in ocular tumor and metastasis

Key words: Plasminogen activator inhibitor-1, angiogenesis, ocular tumor, brain metastasis

Address correspondence to:

Agnès NOEL

University of Liège

Laboratory of Tumor Biology and Development

Institute of Pathology CHU-B23

B-4000 Liège- Sart-Tilman

Belgium

Tel.: +32 4 366 25 68

Fax: +32 4 366 29 36

E-mail: [agnes.noel@ulg.ac.be](mailto:agnes.noel@ulg.ac.be)

## Abstract

Plasminogen activator inhibitor-1 is known to play a paradoxical positive role in tumor angiogenesis, but its contribution to metastatic spread remains unclear. We studied the impact of PAI-1 deficiency in a transgenic mouse model of ocular tumors originating from retinal epithelial cells and leading to brain metastasis (TRP-1/SV40 Tag mice). PAI-1 deficiency did not affect primary tumor growth or vascularization, but was associated with a smaller number of brain metastases. Brain metastases were found to be differentially distributed between the two genotypes. PAI-1-deficient mice displayed mostly secondary foci expanding from local optic nerve infiltration, whereas wild-type animals displayed more disseminated nodules in the scissura and meningeal spaces. SuperArray GEMArray analyses aiming to detect molecules potentially compensating for PAI-1 deficiency demonstrated an increase in fibroblast growth factor-1 (FGF-1) gene expression in primary tumors, which was confirmed by RT-PCR and western blotting. Our data provide the first evidence of a key role for PAI-1 in a spontaneous model of metastasis, and suggest that angiogenic factors, such as FGF-1, may be important for primary tumor growth and may compensate for the absence of PAI-1. They identify PAI-1 and FGF-1 as important targets for combined anti-tumor strategies.

## Introduction

Angiogenesis — the formation of new blood vessels — is an important rate-limiting step during tumor growth and metastatic dissemination. This process requires the coordinated regulation of adhesive, proteolytic and migrating events involving different proteolytic systems. Many clinical studies have established a correlation between adverse outcome in patients with multiple cancer types and high levels of serine proteases of the plasminogen activator (PA) system (for review, see Andreasen *et al.*, 1997). The urokinase-type (uPA) and tissue-type (tPA) plasminogen activators (Rakic *et al.*, 2003). Both uPA and tPA are inhibited by several serine protease inhibitors (SERPINs) including plasminogen activator inhibitor-1 (PAI-1), PAI-2, PAI-3 (protein C inactivator), protease nexin-1 (PN-1) and mammary serine protease inhibitor (Maspin) (Potempa *et al.*, 1994; Rakic *et al.*, 2003). In addition to its inhibitory role during PA-mediated proteolysis, PAI-1 also interacts with vitronectin involved in cell adhesion and migration (Stefansson and Lawrence, 1996; Deng *et al.*, 2001), and LRP (low-density lipoprotein receptor-related protein implicated in the endocytosis of cell surface molecules (Czekay and Loskutoff, 2004; Balsara *et al.*, 2006).

As an inhibitor of uPA, PAI-1 was long thought to be an inhibitor of tumorigenesis and angiogenesis. However, a number of clinical studies reported a correlation between PAI-1 overexpression in human tumors and a poor prognosis (Andreasen *et al.*, 1997; Duffy, 2004). A dose-dependent effect of PAI-1 on pathological angiogenesis has been observed both *in vitro* (Devy *et al.*, 2002) and *in vivo* (Lambert *et al.*, 2003; McMahon *et al.*, 2001; Stefansson *et al.*, 2001; Bajou *et al.*, 2004). Tumor growth and angiogenesis are impaired in mice with a PAI-1 gene deletion (Bajou *et al.*, 1998; Gutierrez *et al.*, 2000; Maillard *et al.*, 2005) or following the induction of PAI-1 expression at supraphysiological levels by adenoviral gene transfer or tumor cell transfection, the administration of recombinant PAI-1 protein and in

transgenic mice overexpressing PAI-1 (Soff *et al.*, 1995; Praus *et al.*, 1999; Ma *et al.*, 1997; McMahon *et al.*, 2001; Bajou *et al.*, 2004).

The impact of PAI-1 on metastatic dissemination is less clear. An increase in pulmonary metastasis has often been observed in response to PAI-1 administration (Tsuchiya *et al.*, 1997). However, other studies have reported no difference in metastatic dissemination with PAI-1 level (Eitzman *et al.*, 1996). These data obtained after induction of experimental tumors by massive tumor cell injection may not be representative of events in the pathogenesis of real cancers. Genetically engineered mouse models that spontaneously develop cancer in a target organ may thus provide a powerful tool for more accurately mimicking the natural history of cancer. A single study has evaluated the impact of PAI-1 deficiency in a transgenic mouse model of cancer (Almholt *et al.*, 2003). Primary breast tumor development and lung metastasis were similar in MMTV-PyMT mice with and without PAI-1 expression (Almholt *et al.*, 2003). It remains unclear whether possible compensatory or redundant mechanisms can mediate tumor angiogenesis and metastatic dissemination in the absence of PAI-1. We backcrossed PAI-1-deficient mice with TRP-1/SV40 Tag transgenic mice, which spontaneously develop ocular tumors derived from retinal pigmented epithelium (RPE), leading to brain metastasis (Penna *et al.*, 1998). We provide evidence that PAI-1 deficiency has no effect on primary ocular tumor growth, but reduces brain metastasis. This report provides the first demonstration that PAI-1 contributes to the early steps of metastatic dissemination in a transgenic mouse tumor model recapitulating all the steps of metastasis. Attempts to identify molecules potentially compensating for PAI-1 deficiency demonstrated increase in levels of mRNA and protein for fibroblast growth factor-1 (FGF-1) in primary tumors.

## Materials and methods

### ***Genetically modified mice***

TRP-1/SV40 Tag transgenic mice were generated by insertion into Y chromosome of a 1.4 kb fragment of tyrosine-related protein 1 (TRP-1) promoter fused to SV40 Tag transforming sequence (Penna *et al.*, 1998). Female PAI-1-deficient mice (PAI-1<sup>-/-</sup>) (Bajou *et al.*, 1998) were mated with male TRP-1/SV40 Tag transgenic mice. F1 males heterozygous for both genes were backcrossed either with PAI-1<sup>-/-</sup> females or with the corresponding wild-type control (WT). All animals used were maintained under specific pathogen-free conditions, with a 12 h light/12 h dark cycle and free access to food and water.

### ***Tissue sample collection and brain metastasis analysis***

For histological analysis, animals were killed 64 days after birth. The entire head of each animal was fixed in 4% formalin. After overnight decalcification (Sakura Finetek, Zoeterwoude, The Netherlands), tissue samples were rinsed in water for 1 h and incubated in 4% formalin for 1 h. Five frontal fragments of the head were cut to isolate several brain areas covering the entire organ. Paraffin sections cut from each head fragment (5 per animal) were stained with hematoxylin and eosin. Total number of metastases per mouse was determined as the number of metastatic foci on 5 sections for each animal (n=22 for PAI-1<sup>-/-</sup> and n=19 for WT mice). Incidence of metastasis was calculated as the percentage of mice with one or more metastatic nodules in the brain. Metastasis severity was scored as: minimal (score 0 = no metastatic nodule), medium (score 1 = less than 4 metastatic nodules), or extensive involvement (score 2 = 5 to 7 metastatic nodules).

### ***Gene array***

Total RNA was extracted from the eyes of 10 TRP-1/PAI-1<sup>-/-</sup> and 9 control TRP-1/PAI-1<sup>+/+</sup> mice (2 month-old), using High Pure RNA isolation kit (Roche Diagnostics, Mannheim, Germany). Relative mRNA expression levels were determined for genes involved in tumor progression and cancer metastasis, using the GEarray (SuperArray Inc., Frederick, MD), according to manufacturer's protocol. Array images were digitized by densitometric scanning on a Fluor-S MultiImager (Bio-Rad Laboratories, Hercules, CA) and analysed by using GEArray Expression Analysis Suite software (SuperArray). Values were normalized with respect to the signal for a housekeeping gene (*GAPDH*). Genes were considered to be differentially expressed if the ratio between control and PAI-1<sup>-/-</sup> mice was greater than 1.5.

### ***Reverse Transcriptase-PCR analysis***

RT-PCR amplification was carried out with the GeneAmp ThermoStable rTth reverse transcriptase RNA PCR kit (Perkin Elmer Life Sciences, Boston, MA) with specific pairs of primers (Table I). RT-PCR products were resolved by electrophoresis in 10% polyacrylamide gels and analyzed with a Fluor-S MultiImager after staining with Gelstar dye (FMC BioProducts, Heidelberg, Germany). RT-PCR products were quantified by normalization with respect to 28S rRNA.

### ***Western blotting***

Entire eyes collected on day 64 were placed in lysis tubes (MagNA Lyser Green Beads, Roche Diagnostics) containing 300 µl of lysis buffer (50 mM Tris/HCl, pH 7.5; 110 mM

NaCl; 10 mM EDTA; 5 mM iodoacetamide; 0.1% NP40). Protein extracts were collected by centrifugation at 12,000 rpm, at 4°C for 30 minutes. Protein concentration was determined with DC Protein Assay Kit (Bio-Rad Laboratories, Hercules, CA). Samples (30 µg of protein) were resolved by SDS-PAGE in 15% polyacrylamide gels under reducing conditions and proteins were transferred to PVDF membranes (NEN, Boston, MA). Membranes were incubated for 2 h in blocking TBS buffer (25 mM Tris/HCl, pH7.6; 150 mM NaCl, 0.1% Tween 20) supplemented with 5% nonfat milk powder. They were then incubated overnight with a polyclonal goat antibody directed against human FGF-1 (R&D systems, Minneapolis). Membranes were washed and incubated for 1h with secondary horseradish peroxidase-conjugated rabbit anti-goat antibody (DAKO, Glostrup, Denmark). Signals were detected with an enhanced chemiluminescence (ECL) kit (Perkin Elmer Life Sciences, Boston) according to manufacturer's instructions. GAPDH detection was carried out (using a rabbit Ab, R&D systems) on the same membranes, as a control.

### ***Statistical analysis***

Statistical differences between experimental groups were assessed with Mann-Whitney test. Chi-squared analysis was used to compare metastasis incidence between groups. Log rank tests were used to compare survival curves. Prism 4.0 software (GraphPad, San Diego, CA) was used and *P*-values < 0.05 were considered significant.

## Results

### ***PAI-1 gene deficiency does not prevent the development of primary ocular tumors***

Primary ocular tumor development was monitored at day 64 after birth in a cohort of TRP-1 PAI-1<sup>-/-</sup> (n=22) and TRP-1 PAI-1<sup>+/+</sup> (WT, n=19) mice (Figure 1A,B). In mice of both genotypes, the entire eyeball and optic nerves were filled by cuboidal neoplastic cells arranged in a tubular fashion, similar to that observed in human carcinomas of the retinal pigmentary epithelium (RPE) (Penna *et al.*, 1998). No difference in tumor histology or vascularization was observed between the two experimental groups (data not shown).

### ***The development of brain metastases is delayed in PAI-1 knockout mice***

Brain metastases developed in 100 % of two-month old TRP-1 transgenic mice. They were quantified by cutting the head of each mouse (n = 22 for PAI-1<sup>-/-</sup> and n=19 for WT mice) frontally into five distinct fragments. Sections (5  $\mu$ m) were prepared from each fragment and metastasis nodules were counted on each slide (5 per animal). Since brain metastases occurred preferentially at three sites, the distribution of metastases (disseminated foci *versus* local foci expanding from optic nerve invasion) was also analyzed (Figure 2).

For all secondary nodules detected in the brain, both the incidence (percentage of animals with metastases) and severity (number of metastatic nodules per animal) of metastases were affected by PAI-1 deficiency. PAI-1-deficient mice had fewer secondary lesions than corresponding WT mice. The mean number of metastases per animal was 2.5  $\pm$  0.3 nodules in PAI-1<sup>-/-</sup> *versus* 3.7  $\pm$  0.5 nodules in WT mice (p=0.02) (Figure 3A). In the absence of PAI-1, 14 % of mice did not display metastasis (severity 0), whereas 100% of WT animals



showed brain metastases (Figure 4). Severity 2 (more than 5 nodules per mouse) metastasis was observed in 37% of WT animals, but in none of the PAI-1<sup>-/-</sup> transgenic mice (Figure 4) ( $p < 0.01$ ).

The main localization of secondary foci was brain parenchyma basis where optic nerves infiltrated by tumor cells come into close contact with brain parenchyma (I in Figure 2A and 2B). These nodules correspond to local invasion through optic nerve infiltration rather than to distant metastases. Metastatic nodules were found in scissura or meningeal spaces (II in Figure 2A and 2C) and in the anterior part of the brain, between the two olfactory lobes (III in Figure 2A and 2D). These three topographic distributions were frequently found in control mice. In sharp contrast, most of the secondary foci in PAI-1-deficient animals expanded from the brain base through optic nerve infiltration, with other distant nodules found only rarely. Indeed, WT mice developed significantly more disseminated brain nodules than did PAI-1 knockout animals (1.7  $\pm$  0.3 nodules in WT *versus* 1  $\pm$  0.2 nodules in PAI-1<sup>-/-</sup> mice,  $p = 0.03$ ) (Figure 3B and C).

Metastatic brain invasion led to animal death. Transgenic PAI-1<sup>-/-</sup> mice had fewer brain metastases, but survival was not affected by PAI-1 status. The median survival was 95 days for PAI-1<sup>-/-</sup> mice and 92.5 days for WT mice (data not shown).

### ***Expression patterns of several factors during tumor follow-up***

As PAI-1 deficiency delayed the development of brain metastasis but did not influence primary tumor progression in the TRP-1/SV40 Tag line, we hypothesized that other components of related proteolytic systems might compensate for the absence of PAI-1. The expression of genes encoding several protease-related candidates was evaluated by semi-quantitative RT-PCR analysis on primary ocular tumors. The molecules studied included components of the plasminogen/plasmin system (tPA, uPA, uPAR, PAI-1, PAI-2, PN-1 and MASPIN), several members of metalloproteinase family putatively involved in angiogenesis (MMP-2, MMP-9, MMP-13 and MMP-14) and their inhibitors (TIMP-1, TIMP-2, TIMP-3 and RECK), and the most important known angiogenic factor, VEGF-A. PAI-1 expression levels were used as an internal control. All the factors studied displayed similar levels of expression in presence and absence of PAI-1, with the exception of TIMP-2 for which larger amounts of mRNA were produced in PAI-1<sup>-/-</sup> mice than in WT mice (0.92 +/- 0.05 arbitrary units in knockout mice *versus* 0.76 +/- 0.02 in WT mice, p=0.005) (Table II).

We extended this expression profiling, using a GEarray containing 96 cDNA fragments printed in quadruplicate (tetra-spots) on a nylon membrane. We identified four genes upregulated by a factor of 1.8 to 2.2 in KO mice: FGF-1, Mucin-1, Ncam-1 and TIMP-2 (Table II). Array verification by semi-quantitative RT-PCR on samples identical to those used for array analysis confirmed the upregulation of FGF-1 (p=0.001) and TIMP-2 (p=0.05) mRNA levels in PAI-1-deficient animals, but not that of Ncam-1 and Mucin-1 levels (Figure 5).

TIMP-2 protein levels were shown, by ELISA, to be similar in TRP-1 PAI-1-deficient and -proficient mice (p=0.7, data not shown). In contrast, levels of FGF-1 production,

assessed by western blotting, were higher in ocular tumors of TRP-1 PAI-1<sup>-/-</sup> mice than in those of their controls ( $p=0.008$ , Figure 6).

## Discussion

Evidence is accumulating that PAI-1 is a potent regulator of angiogenesis and tumor growth (Rakic *et al.*, 2003; Lee and Huang, 2005). Animal tumor models have contributed to characterize PAI-1 functions during tumor development. Nevertheless, conflicting results have been obtained, possibly due to the great diversity of experimental models used (tumor type, number of tumor cells, implantation site) and dose-dependent PAI-1 effects. Further studies in spontaneous carcinogenesis models are required. We investigated the contribution of PAI-1 to spontaneous metastasis, using a model of ocular carcinogenesis including all stages of cancer progression and metastasis formation. By crossing a PAI-1-null allele into TRP-1 mice, we provide the first evidence that PAI-1 contributes to distant metastases in a transgenic tumor model and that increases in the production of an angiogenic factor, FGF-1, might account for similar primary tumor growth in PAI-1-deficient and -proficient mice.

Primary tumor growth and vascularization were found to be similar in PAI-1-proficient and -deficient mice. However, this does not exclude the possibility that PAI-1 contributes to earlier steps in cancer progression. We previously showed, in murine and human skin carcinomas (Bajou *et al.*, 1998; Bajou *et al.*, 2001; Maillard *et al.*, 2005), that PAI-1 is a pro-angiogenic factor and a crucial determinant of tumor microenvironment regulating early stages of primary tumor implantation and growth. However, once the tumor has developed, PAI-1 is no longer essential for cancer progression (Maillard *et al.*, 2005). Accordingly, PAI-1 deficiency does not affect primary tumor development in MMTV-PyMT model (Almholt *et al.*, 2003). The similar development of primary tumors in both genotypes allowed unbiased comparison of metastases. We show here that PAI-1 deficiency is associated with smaller numbers of brain metastases. We also found that the distribution of metastases was different in PAI-1<sup>+/+</sup> and PAI-1<sup>-/-</sup> brains. Secondary foci in PAI-1<sup>-/-</sup> mice were mostly derived from

local infiltration of optic nerves, expanding toward brain parenchyma, whereas more distant metastatic foci were detected in the scissura and meningeal spaces of WT animals. This constitutes the first demonstration that PAI-1 deficiency affects metastatic dissemination in a model of spontaneous carcinogenesis.

A possible explanation for the lack of effect of PAI-1 deficiency on the growth of primary TRP-1/SV40 Tag eye tumors is a functional overlap between PAI-1 and other protease inhibitors. We therefore searched for functional redundancy, focusing on alternative inhibitors of matrix remodeling (PAI-2, PN-1, Maspin, TIMPs) and other compounds of PA and MMP proteolytic systems putatively involved in angiogenesis. Such a functional overlap between MMP and PA systems has been demonstrated in wound healing (Lund *et al.*, 1999). However, our transgenic tumor model provided no evidence that PAI-1 deficiency led to functional redundancy or a compensatory increase in the levels of proteases or their inhibitors. By using a more global approach based on Superarray GEarray technology, increased FGF-1 production in primary tumors was detected at mRNA levels and confirmed at protein levels. FGF-1 is not only angiogenic, but also acts as an important survival factor for normal RPE cells or endothelial cells (Bryckaert *et al.*, 2000; Guillonneau *et al.*, 1997; Uriel *et al.*, 2006). FGF-1 therefore probably promotes primary RPE tumor growth and angiogenesis through several mechanisms.

There is an apparent discrepancy between the dramatic effects of PAI-1 deficiency in transplanted human and murine tumor models (Bajou *et al.*, 1998; Gutierrez *et al.*, 2000; Maillard *et al.*, 2005; Lee and Huang, 2005) and the absence of an impact on spontaneous tumor development in carcinogenesis models, such as MMTV-PyMT (Almholt *et al.*, 2003) and TRP-1/SV40 Tag transgenic mice. One possible reason is that compensatory mechanisms, such as angiogenic molecule production, can take place in transgenic mice during development and growth, but not in mice challenged by massive tumor cell injections.

The higher levels of FGF-1 production observed in TRP-1/SV40 Tag tumors was not detected in the skin transplantation model used in previous studies (Bajou *et al.*, 1998) (data not shown). This suggests that FGF-1 overproduction may be specific to RPE tumors or take place throughout pathological angiogenesis, as a host response, and not during transient challenge. Carcinogenesis models thus better reflect the real pathogenesis of cancer and may provide important information regarding host reaction to the long-term inhibition or deletion of a specific gene product.

PAI-1 is a multifunctional protein. In addition to its serpin function, it also binds to vitronectin, thereby regulating cell adhesion and migration (Czekay and Loskutoff, 2004). This protein also has a LRP binding site involved in controlling cell migration via uPA/uPAR internalization (Herz and Strickland 2001) and in regulating cell proliferation and apoptosis via the PI3K/AKT pathway (Balsara *et al.*, 2006). To dissect functional properties of PAI-1, we and others have used mutated forms of rPAI-1 that unraveled novel PAI-1 activities unrelated to serine protease-inhibitory activity (Bajou *et al.*, 2001; Lambert *et al.*, 2003; Praus *et al.*, 2002; Stefansson *et al.*, 2001; Balsara *et al.*, 2006). However, this strategy is hampered in the present model, by the occurrence of tumor transformation and progression *in utero* and the impossibility of using adenovirus-mediated gene transfer or recombinant protein injection at early stages. In addition, the anatomy of the eye hinders the access of pharmacological compounds to intraocular environment in neonatal or adult mice (Bouquet *et al.*, 2003).

Pharmacological compounds modulating PAI-1 activities are currently under development (Leik *et al.* 2006; Liang *et al.* 2005). However, particular features of PAI-1 might raise concerns about its targeting for treatment purposes and should be carefully addressed: 1) its multifunctionality, 2) its short half-life *in vivo*, 3) its dose-dependent effect, and finally 4) its impact on the fibrinolytic system and on the process of atherosclerosis and thrombosis. A strategy based on the use of specific stabilized mutants interfering with binding

to vitronectin, but without affecting PA activity, can be used to block angiogenesis without affecting fibrinolysis or thrombosis (Stefansson *et al.*, 2001). Despite major progress toward the development of pharmacological PAI-1 inhibitors, there is currently no evidence to suggest that compensatory mechanisms are induced following the deletion or long-term inhibition of PAI-1. Our study provides the first evidence of an increase in FGF-1 production in the absence of PAI-1 gene. This may account for the lack of a phenotype in the development of primary tumors in PAI-1-deficient mice and may, at least partly, account for some of the conflicting data reported in previous studies. Our data highlight the need for further investigations before the clinical use of PAI-1-targeting compounds. The recent approval of anti-angiogenic agents for clinical applications has not only provided a proof-of-concept for anti-angiogenic strategies, but has also highlighted the possible progressive emergence of resistance to treatment (Carmeliet, 2005). Our data suggest that the long-term targeting of PAI-1 might be counteracted by the overproduction of angiogenic factors, such as FGF-1. Further studies, in other models, are urgently required to address this important issue.

## Legends to figures

### **Figure 1**

Frontal sections (5  $\mu$ m) of the head crossing the middle of the eyes, from TRP-1 WT (A) and TRP-1 PAI-1 knockout (PAI-1<sup>-/-</sup>) mice (B). Mice were killed 64 days after birth and histological sections were stained with hematoxylin and eosin (H&E). E, primary eye tumor; ON, optic nerve; B, Brain. Original magnification: 10x. Bars, 2 mm.

### **Figure 2**

Localization of metastasis in the brain. A: Schematic sagittal section of the head visualizing the three preferential sites of metastases (I, II and III). B, C and D: Frontal brain sections stained with hematoxylin and eosin. Tumor cells invading optic nerves formed nodules in the brain parenchyma adjacent to these nerves (I in panels A and B). Some metastases disseminated in the meningeal spaces (II in panels A and C). Nodules were also detected between the two olfactory lobes in frontal sections crossing the eyes (III in panels A and D).

### **Figure 3**

Quantification of brain metastases in TRP-1 PAI-1<sup>-/-</sup> and TRP-1 control animals. TRP-1 PAI-1<sup>+/+</sup> (WT, ■, n=19) and TRP-1 PAI-1<sup>-/-</sup> (▲, n=22) mice were killed 64 days after birth. For each animal, nodules were counted on five different brain sections stained with H&E, to obtain a total number of metastases per animal (A). Disseminated nodules were quantified by counting the total number of nodules in the anterior part of the brain (between the 2 olfactory lobes) and in meningeal spaces (B) (see the legend to figure 2). Nodules expanding from optic nerves correspond to the infiltration of 1 or 2 optic nerves and propagation to close cerebral parenchyma (C). Horizontal bars represent median values, *P*-values correspond to the Mann-Whitney test (\* *P* ≤ 0.05; NS, non significant value).



#### **Figure 4**

Severity of brain metastases. The severity of metastases was determined as described in materials and methods. Severity 0: no detectable metastases; severity 1: 1 to 4 nodules per mouse; severity 2: more than 5 metastases per mouse. Chi-squared analysis was carried out ( $P < 0.01$ ).

#### **Figure 5**

Gene array verification by semi-quantitative RT-PCR analysis. Total RNA was extracted from eye tumors of 11 TRP-1 PAI-1-deficient and 9 TRP-1 control mice killed on day 64. Levels of 28S rRNA (A) and PAI-1 mRNA (B) were assessed as controls. For each PCR product studied (B: PAI-1, C: FGF-1, D: Mucin-1, E: Ncam-1 and F: TIMP-2), the upper panel shows a representative polyacrylamide gel with 6 representative samples from WT (left part) and PAI-1 KO mice (right part). The expected sizes of amplified products are indicated on the right. Scatter plots (below panels) correspond to the densitometric quantification of PCR products. Results are expressed as amplified mRNA level divided by 28S ribosomal RNA level. Horizontal bars indicate mean values,  $P$ -values correspond to Mann-Whitney tests (\*  $P \leq 0.05$ ; \*\*\*  $P \leq 0.005$ ; NS, non significant).

#### **Figure 6**

Western blot analysis of FGF-1 production in TRP-1 transgenic mice with and without deletion of PAI-1 gene. A: Western-blot analysis of 3 representative samples from WT and PAI-1<sup>-/-</sup> mice. Recombinant human (rh) FGF-1 was used as positive control. GAPDH protein levels were assessed as a loading control. B: quantification of FGF-1 production by scanning densitometry in WT (white bars) and PAI-1<sup>-/-</sup> (black bars) mice. Results are expressed as

FGF-1 protein levels divided by GAPDH protein levels. *P*-values indicated correspond to Mann-Whitney test.

## Acknowledgments

We thank E. Connault, I. Dasoul, E. Feyereisen, E. Konradowski, M.R. Pignon and F. Olivier for excellent technical assistance.

This work was supported by grants from the Commission of European Communities (FP6 : LSHC-CT-2003-503297, LSHC-CT-2004-503224), Fonds de la Recherche Scientifique Médicale, Fonds National de la Recherche Scientifique (F.N.R.S., Belgium), Fédération Belge Contre le Cancer, C.G.R.I.-F.N.R.S.-INSERM Coopération, the Fonds spéciaux de la Recherche (University of Liège), Centre Anticancéreux près l'Université de Liège, Fondation Léon Fredericq (University of Liège), the D.G.T.R.E. from « Région Wallonne », Interuniversity Attraction Poles Programme - Belgian Science Policy (Brussels, Belgium). CM, MM and MJ are recipients of a grant from FNRS-Télévie.

## References

- Almholt K, Nielsen BS, Frandsen TL, Brunner N, Dano K, Johnsen M. (2003). Metastasis of transgenic breast cancer in plasminogen activator inhibitor-1 gene-deficient mice. *Oncogene* **22**: 4389-4397.
- Andreasen PA, Kjoller L, Christensen L, Duffy MJ. (1997). The urokinase-type plasminogen activator system in cancer metastasis: a review. *Int J Cancer* **72**: 1-22.
- Bajou K, Maillard C, Jost M, Lijnen RH, Gils A, Declerck P, *et al.* (2004). Host-derived plasminogen activator inhibitor-1 (PAI-1) concentration is critical for in vivo tumoral angiogenesis and growth. *Oncogene* **23**: 6986-6990.
- Bajou K, Masson V, Gerard RD, Schmitt PM, Albert V, Praus M, *et al.* (2001). The plasminogen activator inhibitor PAI-1 controls in vivo tumor vascularization by interaction with proteases, not vitronectin. Implications for antiangiogenic strategies. *J Cell Biol* **152**: 777-784.
- Bajou K, Noel A, Gerard RD, Masson V, Brunner N, Holst-Hansen C, *et al.* (1998). Absence of host plasminogen activator inhibitor 1 prevents cancer invasion and vascularization. *Nat Med* **4**: 923-928.
- Balsara RD, Castellino FJ, Ploplis VA. (2006). A novel function of plasminogen activator inhibitor-1 in modulation of the AKT pathway in wild-type and plasminogen activator inhibitor-1-deficient endothelial cells. *J Biol Chem* **281**: 22527-22536.
- Bouquet C, Frau E, Opolon P, Connault E, Abitbol M, Griscelli F, *et al.* (2003). Systemic administration of a recombinant adenovirus encoding a HSA-Angiostatin kringle 1-3

conjugate inhibits MDA-MB-231 tumor growth and metastasis in a transgenic model of spontaneous eye cancer. *Mol Ther* **7**: 174-184.

Bryckaert M, Guillonneau X, Hecquet C, Perani P, Courtois Y, Mascarelli F. (2000). Regulation of proliferation-survival decisions is controlled by FGF1 secretion in retinal pigmented epithelial cells. *Oncogene* **19**: 4917-4929.

Carmeliet P. (2005). Angiogenesis in life, disease and medicine. *Nature* **438**: 932-936.

Czekay RP, Loskutoff DJ. (2004). Unexpected role of plasminogen activator inhibitor 1 in cell adhesion and detachment. *Exp Biol Med (Maywood.)* **229**: 1090-1096.

Deng G, Curriden SA, Hu G, Czekay RP, Loskutoff DJ. (2001). Plasminogen activator inhibitor-1 regulates cell adhesion by binding to the somatomedin B domain of vitronectin. *J Cell Physiol* **189**: 23-33.

Devy L, Blacher S, Grignet-Debrus C, Bajou K, Masson V, Gerard RD, *et al.* (2002). The pro- or antiangiogenic effect of plasminogen activator inhibitor 1 is dose dependent. *FASEB J* **16**: 147-154.

Duffy MJ. (2004). The urokinase plasminogen activator system: role in malignancy. *Curr Pharm Des* **10**: 39-49.

Eitzman DT, Krauss JC, Shen T, Cui J, Ginsburg D. (1996). Lack of plasminogen activator inhibitor-1 effect in a transgenic mouse model of metastatic melanoma. *Blood* **87**: 4718-4722.

Guillonneau X, Regnier-Ricard F, Dupuis C, Courtois Y, Mascarelli F. (1997). FGF2-stimulated release of endogenous FGF1 is associated with reduced apoptosis in retinal pigmented epithelial cells. *Exp Cell Res* **233**: 198-206.

Gutierrez LS, Schulman A, Brito-Robinson T, Noria F, Ploplis VA, Castellino FJ. (2000). Tumor development is retarded in mice lacking the gene for urokinase-type plasminogen activator or its inhibitor, plasminogen activator inhibitor-1. *Cancer Res* **60**: 5839-5847.

Herz J, Strickland DK. (2001). LRP: a multifunctional scavenger and signaling receptor. *J Clin Invest* **108**: 779-784.

Lambert V, Munaut C, Carmeliet P, Gerard RD, Declerck PJ, Gils A, *et al.* (2003). Dose-dependent modulation of choroidal neovascularization by plasminogen activator inhibitor type I: implications for clinical trials. *Invest Ophthalmol Vis Sci* **44**: 2791-2797.

Lee CC, Huang TS. (2005). Plasminogen Activator Inhibitor-1: The expression, biological functions, and effects on tumorigenesis and tumor cell adhesion and migration. *Journal of Cancer Molecules* **1**: 25-36.

Leik CE, Su EJ, Nambi P, Crandall DL, Lawrence DA. (2006). Effect of pharmacologic plasminogen activator inhibitor-1 inhibition on cell motility and tumor angiogenesis. *J Thromb Haemost* **4**: 2710-2715.

Liang A, Wu F, Tran K, Jones SW, Deng G, Ye B, *et al.* (2005). Characterization of a small molecule PAI-1 inhibitor, ZK4044. *Thromb Res* **115**: 341-350.

Lund LR, Romer J, Bugge TH, Nielsen BS, Frandsen TL, Degen JL, *et al.* (1999). Functional overlap between two classes of matrix-degrading proteases in wound healing. *EMBO J* **18**: 4645-4656.

Ma D, Gerard RD, Li XY, Alizadeh H, Niederkorn JY. (1997). Inhibition of metastasis of intraocular melanomas by adenovirus-mediated gene transfer of plasminogen activator inhibitor type 1 (PAI-1) in an athymic mouse model. *Blood* **90**: 2738-2746.

Maillard C, Jost M, Romer MU, Brunner N, Houard X, Lejeune A, *et al.* (2005). Host plasminogen activator inhibitor-1 promotes human skin carcinoma progression in a stage-dependent manner. *Neoplasia* **7**: 57-66.

McMahon GA, Petitclerc E, Stefansson S, Smith E, Wong MK, Westrick RJ, *et al.* (2001). Plasminogen activator inhibitor-1 regulates tumor growth and angiogenesis. *J Biol Chem* **276**: 33964-33968.

Penna D, Schmidt A, Beermann F. (1998). Tumors of the retinal pigment epithelium metastasize to inguinal lymph nodes and spleen in tyrosinase-related protein 1/SV40 T antigen transgenic mice. *Oncogene* **17**: 2601-2607.

Potempa J, Korzus E, Travis J. (1994). The serpin superfamily of proteinase inhibitors: structure, function, and regulation. *J Biol Chem* **269**: 15957-15960.

Praus M, Collen D, Gerard RD. (2002). Both u-PA inhibition and vitronectin binding by plasminogen activator inhibitor 1 regulate HT1080 fibrosarcoma cell metastasis. *Int J Cancer* **102**: 584-591.

Praus M, Wauterickx K, Collen D, Gerard RD. (1999). Reduction of tumor cell migration and metastasis by adenoviral gene transfer of plasminogen activator inhibitors. *Gene Ther* **6**: 227-236.

Rakic JM, Maillard C, Jost M, Bajou K, Masson V, Devy L, *et al.* (2003). Role of plasminogen activator-plasmin system in tumor angiogenesis. *Cell Mol Life Sci* **60**: 463-473.

Soff GA, Sanderowitz J, Gately S, Verrusio E, Weiss I, Brem S, *et al.* (1995). Expression of plasminogen activator inhibitor type 1 by human prostate carcinoma cells inhibits primary

tumor growth, tumor-associated angiogenesis, and metastasis to lung and liver in an athymic mouse model. *J Clin Invest* **96**: 2593-2600.

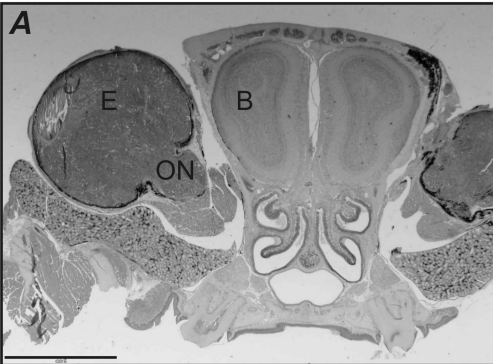
Stefansson S, Lawrence DA. (1996). The serpin PAI-1 inhibits cell migration by blocking integrin alpha V beta 3 binding to vitronectin. *Nature* **383**: 441-443.

Stefansson S, Petitclerc E, Wong MK, McMahon GA, Brooks PC, Lawrence DA. (2001). Inhibition of angiogenesis in vivo by plasminogen activator inhibitor-1. *J Biol Chem* **276**: 8135-8141.

Tsuchiya H, Sunayama C, Okada G, Matsuda E, Tomita K, Binder BR. (1997). Plasminogen activator inhibitor-1 accelerates lung metastasis formation of human fibrosarcoma cells. *Anticancer Res* **17**: 313-316.

Uriel S, Brey EM, Greisler HP. (2006). Sustained low levels of fibroblast growth factor-1 promote persistent microvascular network formation. *Am J Surg* **192**: 604-609.

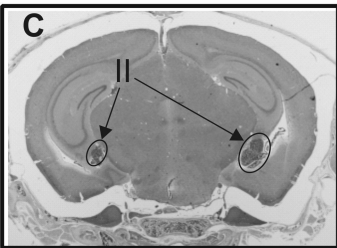
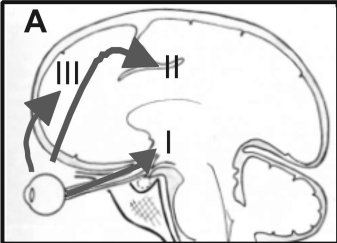
WT



PAI-1 KO







[illegible]

Number of disseminated nodules/animal

WT PAI-1 KO

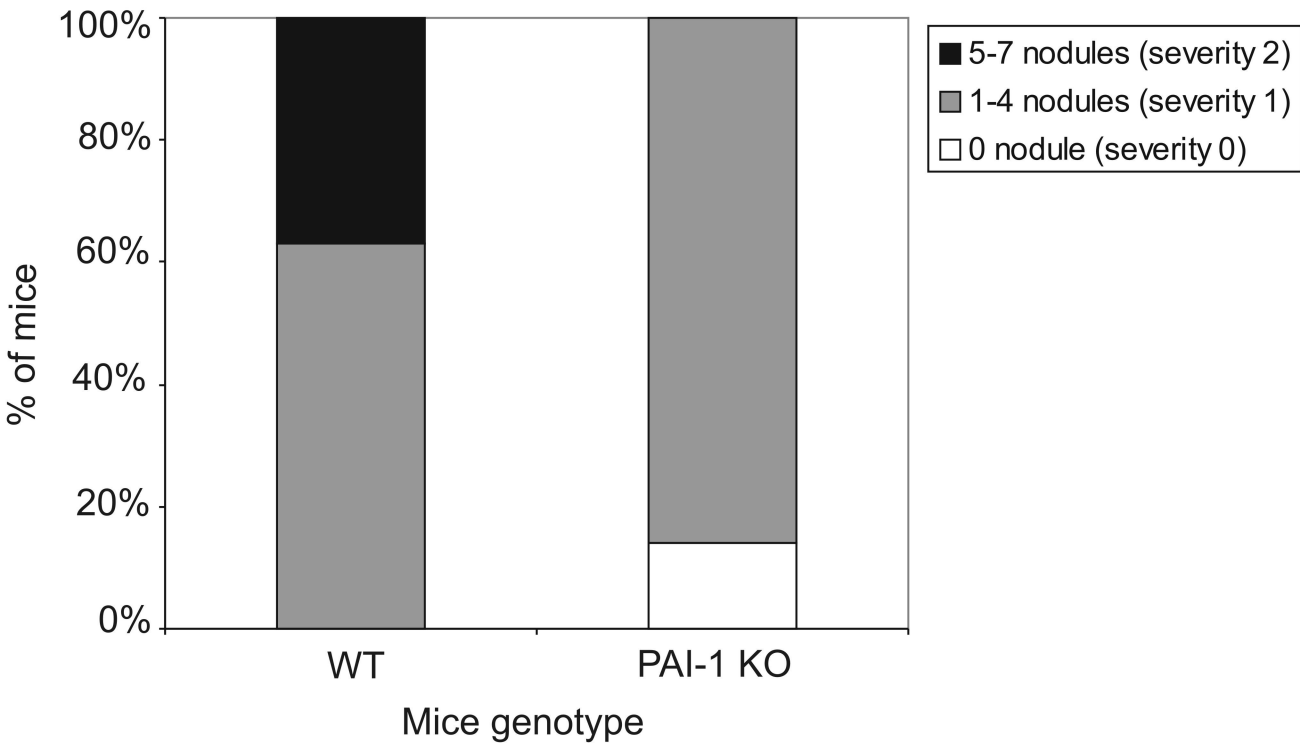
\*

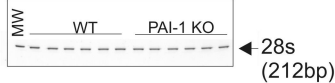
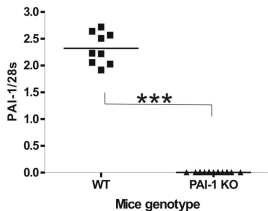
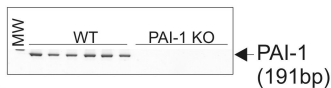
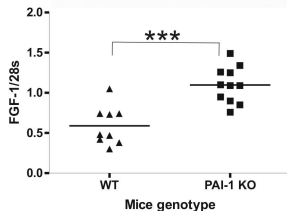
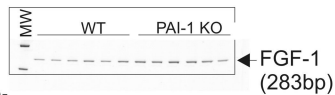
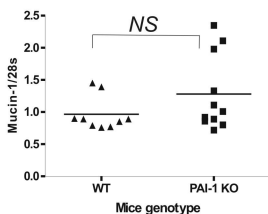
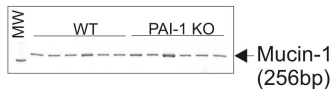
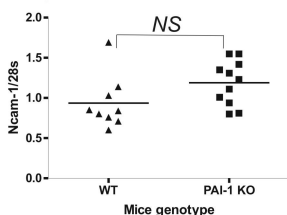
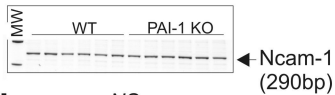
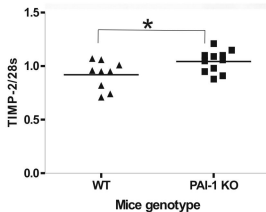
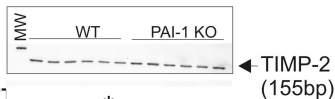
Group	Number of disseminated nodules/animal	Count
WT	0	2
	1	10
	2	3
	3	6
	4	1
PAI-1 KO	0	7
	1	10
	2	5
	3	1

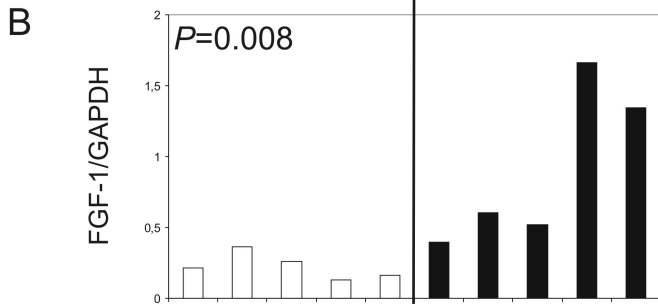
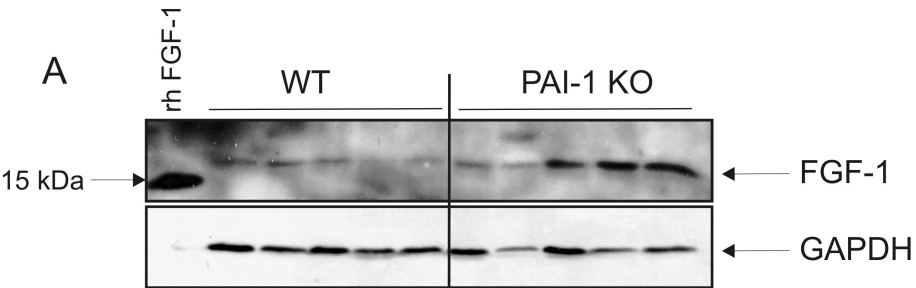
A dot plot comparing the number of nodules expanding from optical nerves per animal between WT and PAI-1 KO mice. The y-axis is labeled "Number of nodules expanding from optical nerves/animal" and ranges from 0 to 5. The x-axis has two categories: "WT" and "PAI-1 KO". Each dot represents one animal. Horizontal lines indicate the mean for each group. A bracket labeled "NS" (Not Significant) spans both groups.

Group	Individual Values (n)	Mean ± SEM
WT	0 (3), 1 (5), 2 (3), 3 (6), 4 (3)	~2.0 ± 0.2
PAI-1 KO	0 (3), 1 (5), 2 (17)	~1.5 ± 0.1

## Mice genotype



**A****B****C****D****E****F**



	Forward primer (5'→3')	Reverse primer (5'→3')	Cycles (n)
MMP-2	5'-AGATCTTCTTCTCAAGGACCGGT-3'	5'-GGCTGGTCAGTGGCTTGGGGTA-3'	27
MMP-9	5'-GCGGAGATTGGGAACCAGCTGTA-3'	5'-GACGCGCCTGTGTACACCCACA-3'	35
MMP-13	5'-ATGATCTTTAAAGACAGATTCTTCTGG-3'	5'-TGGGATAACCTTCCAGAATGTCATAA-3'	33
MMP-14	5'-GGATACCAATGCCCATTGGCCA-3'	5'-CCATTGGGCATCCAGAAGAGAGC-3'	27
TIMP-1	5'-CATCCTGTTGTGCTGTGGCTGAT-3'	5'-GTCATCTTGATCTCATAACGCTGG-3'	30
TIMP-2	5'-CTCGCTGGACGTTGGAGGAAAGAA-3'	5'-AGCCCATCTGGTACCTGTGGTTCA-3'	25
TIMP-3	5'-CTTCTGCAACTCCGACATCGTGAT-3'	5'-CAGCAGGTACTGGTACTTGTGAC-3'	27
RECK	5'-GGCCCTTGCCAGCCTTTCTGCAGA-3'	5'-ACAGCAAGCCCCTGGTGGGATGA-3'	33
uPA	5'-ACTACTACGGCTCTGAAGTCACCA-3'	5'-GAAGTGTGAGACTCTCGTGTAGAC-3'	30
tPA	5'-CTACAGAGCGACCTGCAGAGAT-3'	5'-AATACAGGGCCTGCTGACACGT-3'	27
uPAR	5'-ACTACCGTGCTTCGGGAATG-3'	5'-ACGGTCTCTGTCAGGCTGATG-3'	30
PAI-1	5'-AGGGCTTCATGCCCCACTTCTTCA-3'	5'-AGTAGAGGGCATTCACCAGCACCA-3'	30
PAI-2	5'-CTCAAACCAAAGGTGAAATCCCAA-3'	5'-GGTATGCTCTCATGCGAGTTCACA-3'	30
Maspin	5'-CACAGATGGCCACTTTGAGGACAT-3'	5'-GGGAGCACAATGAGCATACTCAGA-3'	27
PN-1	5'-GGTCCTACCCAAGTTCACAGCTGT-3'	5'-AGGATTGCAGTTGTTGCTGCCGAA-3'	27
VEGF-A	5'-CCTGGTGGACATCTCCAGGAGTA-3'	5'-CTACCCGCCTCGGCTTGTCACA-3'	33
FGF-1	5'-GGCTGAAGGGGAGATCACAACCTT-3'	5'-CATTTGGTGTCTGCGAGCCGTATA-3'	29
Mucin-1	5'-GTGCTGGTCTGTATTTGGTTGCT-3'	5'-GTCACCACAGCTGGGTGGTATAA-3'	27
Ncam-1	5'-GCTATCTGGAGGTGACCCAGATT-3'	5'-CCTCCATGTTGGCTTCTTTGGCAT-3'	27
28s	5'-GTTCACCCATAATAGGGAACGTGA-3'	5'-GATTCTGACTTAGAGGCGTTCAGT-3'	15
<b>Table 1.</b> Sequences of primers used for RT-PCR studies.			

	Semi-quantitative RT-PCR	Gearray
Plasminogen/plasmin system :		
uPA	=	=
tPA	=	=
uPAR	=	=
PAI-1	WT>KO	WT>KO
PAI-2	=	=
PN-1	=	Absent from the membrane
Maspin	=	=
MMPs and their inhibitors :		
MMP-2	=	=
MMP-9	=	=
MMP-14	=	=
MMP-13	=	=
TIMP-1	=	=
TIMP-2	KO>WT	KO>WT
TIMP-3	=	=
RECK	=	Absent from the membrane
Angiogenic factor : VEGF-A	=	=
Other regulated factors :		
FGF-1		KO>WT
Mucin-1		KO>WT
Ncam-1		KO>WT
<b>Table 2.</b> Studies of gene expression by semi-quantitative RT-PCR analysis and Superarray membrane on total RNA extracted from eye tumors of TRP-1 PAI-1 <sup>-/-</sup> (KO) and TRP-1 PAI-1 <sup>+/+</sup> (WT) mice. =, similar expression level; WT>KO, higher expression level in WT than in KO mice; KO>WT, higher expression level in KO than in WT mice.		